Do Wormholes Play A Role In Heavy Oil Cold Production?

Sandy Chen, Larry Lines, and P. F. Daley

2004 CSEG National Convention

Abstract

The simultaneous extraction of oil and sand during the cold production of heavy oil generates high porosity channels termed "wormholes". Wormholes grow in a 3D radial pattern within a certain layer of net pay zones, resulting in the development of a high permeability network in the reservoir, boosting oil recovery. Meanwhile, the development of wormholes causes reservoir pressure to fall below the bubble point, resulting in dissolved-gas coming out of solution to form foamy oil. Amplitude anomalies in the vicinity of the borehole observed in time-lapse seismic survey are possibly a result of the presence of foamy oil and wormholes. The foamy oil effects on seismic responses have been discussed at the CSEG convention of 2003. Here, we address the use of time-lapse reflection seismology to detect the effects of wormholes.

Tremblay et al. (1999) observed in the laboratory experiments that the diameters of wormholes are relatively small, on the order of centimetres, but the porosity of the mature wormholes could reach 50% or more. With porosities greater than the critical porosity within wormholes, both frame and shear moduli of the suspension sands could significantly decrease. The shear modulus tends to zero in the suspension sands. This leads to the decrease of both P-wave and S-wave velocities of the wormhole sands. Although individual wormholes cannot be imaged as their diameters are of the order of centimeters, macroscopic effects of wormholes on P- and S-wave velocities of the reservoir rock can be possibly observed, when large amount of sands are produced, and high dense wormholes exist. 2D numerical models have been designed to examine the footprints of wormholes from both PP and PS seismic data. The modeling results indicate that PS data can better image the wormhole footprints than PP data. The increase of amplitude anomalies appears to be proportional to wormhole density.

Introduction

Cold production of heavy oil is a non-thermal process, in which sand and oil are produced simultaneously. This process has been economically successful in several heavy oil fields in Alberta and Saskatchewan. The extraction of sand creates a wormhole network and a foamy oil drive. These two effects are thought to be the main influences in enhanced oil recovery. The foamy oil effects on seismic responses during heavy oil cold production surveys have been discussed at the 2003 CSEG convention (Chen et al). This paper will focus on the wormhole effects on seismic data.

The cold production process is a pressure driven process, in which both heavy oil and sand are transported to the surface using a progressive cavity pump. This extraction causes high pressure gradients in the reservoir resulting in the failure of the unconsolidated sand matrix. The failed sand flows to the well, triggering the development of wormholes. Sawatzky et al, (2002) believe that wormholes grow in unconsolidated, clean sand layers within the net pay zone, along the highest pressure gradient between the borehole and the tip of the wormhole. These grow in a radial pattern to a distance of 150 m or more from the wells, forming approximately horizontal high permeability, porosity channels in the reservoirs. Laboratory experiments conducted by Alberta Research Council (Tremblay, et al 1999) indicated that the porosity of mature wormholes could reach 50%, and the wormhole diameters could range from the order of 10 cm to one meter (Figure 1).

With porosities greater than the critical porosity, the sands within the wormholes are in a state of suspension. Figure 2 shows a critical porosity ϕ_c of sandstones. The critical porosity is defined as the porosity that separates their mechanical and acoustic behaviour into two distinct domains (Nur, et al 1998). In other words, the critical porosity can be thought of as a critical value to separate the compressibility and rigidity of saturated rocks into two distinct domains, which are frame-supported and fluid-supported domains. Different rocks have their particular critical porosities. Sands within the wormholes are suspended within mixed fluids, including heavy oil, water and foamy oil.
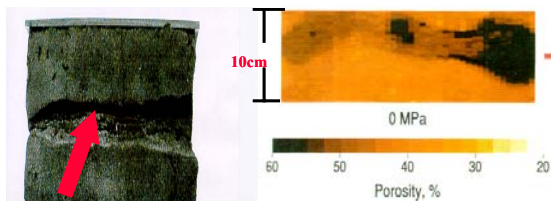

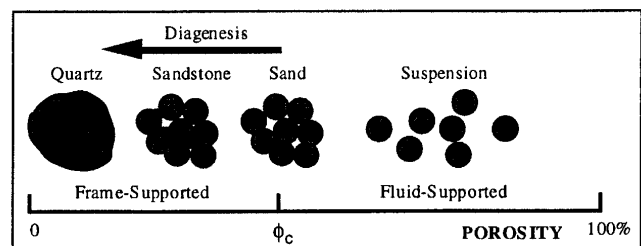Figure 1 Wormholes simulated in reservoir lab (Tremblay, 1999)

Figure 2 Physical meaning of critical porosity (Nur, 1998)

Methodology

In order to compute the compressional and shear moduli of the suspending sands within wormholes, we employed Murphy (1993) 's theory where they believed that the Boit-Gassmann relation remains valid through the consolidation transition at critical porosity ϕ_c. If $\phi > \phi_c$ and the grains are suspended in the fluid, then the frame modulus $K_d=0$, shear modulus $\mu=0$, and bulk modulus K_u is given by Wood's (1941) formula (Reuss Lower Bound). Downton (2001) thought that the bulk modulus and shear modulus of a saturated rock of porosity ϕ will lie between Reuss lower bound and Voigt upper bound. Therefore, the Upper and Lower bounds can be applied to calculating the ranges of bulk and shear moduli of any porous rock.

Murphy et al (1993) also compiled high quality laboratory data on gas saturated, pure quartz sands and sandstones, and established the relations between the frame bulk modulus and shear modulus with porosity. The best empirical relations give the responding values of the frame bulk modulus and shear modulus of sandstone at any porosity.

In this paper, these empirical relations and both lower and upper bounds were applied to the computation of bulk and shear moduli of porous sands using in-situ parameters from the Lloydminster heavy oil field. Here, the foamy oil effects has been minimized.

Figure 3 shows that for porosities less than the critical porosity (here is 35%, from Murphy), the bulk and shear moduli based on the empirical relations lie between the lower and upper bounds with a linear relationship. For porosities greater than the critical porosity, the moduli fit the Reuss lower bound. Specially, the shear moduli tend to be zero when grains are suspended in the fluid.
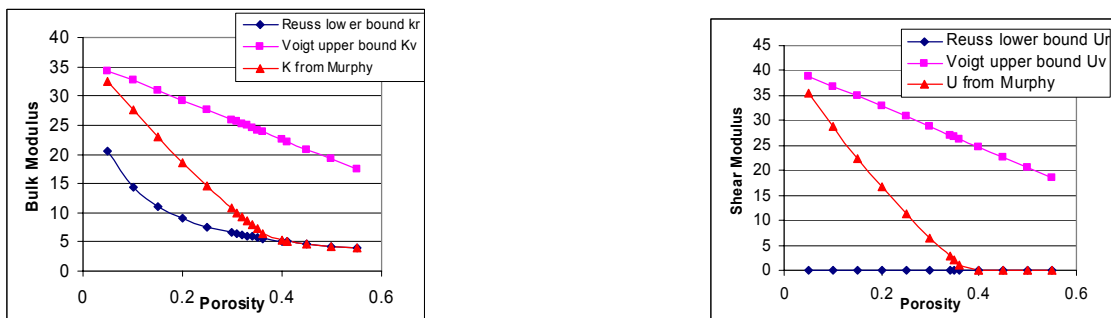

Figure 3 Bulk modulus (left) and shear modulus (right) versus porosity using lower and upper bounds, empirical relations

Since the empirical relations derived by Murphy (1993) properly lie both lower and upper bounds at any porosity, we applied them to calculation of both P-wave and S-wave velocities with the variations of porosity. In Figure 4a, it can be clearly seen that both P-wave and S-wave velocities decrease with the increase of porosity. And the S-wave velocity could approach zero when porosities are greater than the critical porosity.

It is not possible to detect individual wormholes using surface seismic data due to the small diameter of wormholes. However, the macroscopic effects of wormholes on V_p and V_s within the drainage sands (net pay zone) can be probably observed. By comparisons, we think that these macroscopic effects have been reasonably obtained using Voigt upper bound. The reductions of average V_p and V_s of the drainage zone are proportional to the wormhole density, while bulk density ρ hardly changes (shown in Figure 4b). The decrease in V_s appears more rapid than V_p.

(a)

(b)

Figure 4 (a) are velocities vs porosity of porous sands using Murphy's emprical relations; (b) are velocities and density of drainage sands (which is on the microscopic influence of the presence of wormholes) vs. wormhole density, where wormhole density is defined as the percentage of wormhole volume to the entire drainage volume. Here, the wormhole porosity is defined as 50%, reservoir sands porosity as 30%.

Geology and numerical models

Commencement of cold production disturbs the initial reservoir state through the presence of foamy oil and wormholes, modifying the fluid phase and elastic properties within drainage areas (blue coloring area). Again, only the wormhole effects are addressed here. It is assumed that the drainage zone is a 3D cylinder around boreholes. A schematic of this is shown in Figure 5, a 3D map view on the top, and a 2D cross-section at the bottom. The volume of the drainage zone is determined by the length of wormholes and the net pay thickness. Considering the net pay thickness of most cold production reservoir are thin, less than 10m, we assume that wormhole effects on rock properties can overwhelm through the entire pay thickness. The pre-production 2D reservoir numerical model is built based on well logs in a Lloydminster cold production field. Figure 6 only shows the post-production model with one drainage zone, 6m thick, and 200m long. And there is no drainage zone of the pre-production reservoir model. The drainage zone has been divided into 10 lateral blocks. A wormhole density increase from 2% to 20% in adjacent blocks is incorporated, corresponding to V_p varying from 2688m/s to 2478m/s and V_s from 1717m/s to 1404m/s obtained from Figure 4b. The reason to design lateral wormhole density changes is to observe the variations of amplitudes with wormhole denisty changes.
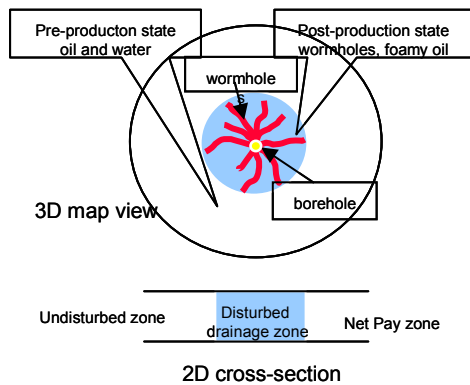

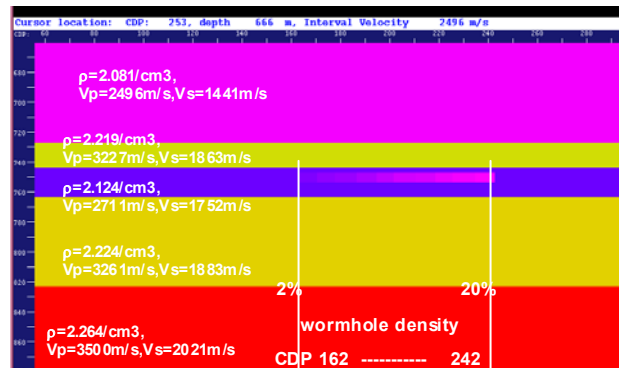Figure 5 Simplified drainage model with foamy

Figure 6 2D post-production geological model with wormhole effects

Modeling results and conclusions

Ray-tracing modeling has been employed using a 60Hz Ricker wavelet to generate synthetic seismograms. Figure 7 shows the stacking sections of PP seismic data of the pre-production reservoir model and the post-production model with the drainage zone, as well as the difference section by subtracting Figure 7a and 7b. In Figure 7b, the drainage zone locates between CDP 162 and 242. Here, slightly amplitude and phase changes can be observed within the drainage zone. The changes can be easier seen around CDP 240, where the higher wormhole density exists, corresponding to larger reflection coefficients. The difference of the amplitudes and phases can be clearly observed in Figure 7c. Also, the traveltime delay can be observed underneath the high wormhole density zone near CDP 240, due to the larger velocity and density contrasts with higher wormhole density.

(a) pre-production reservoir

(b) drainage zone with wormhole effects
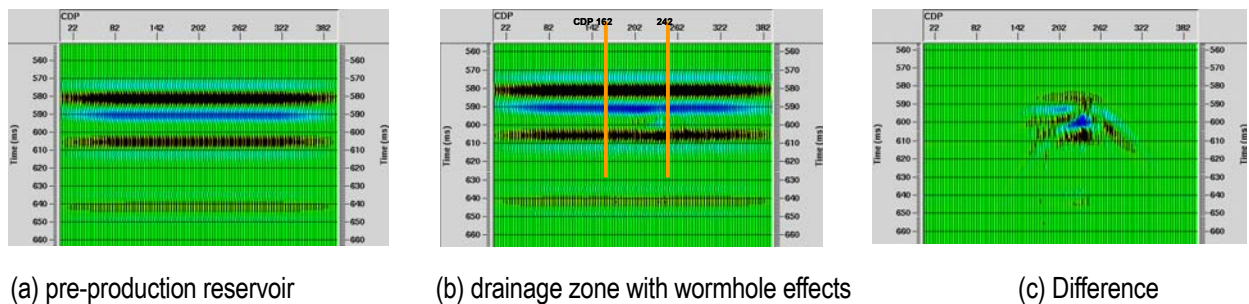

(c) Difference

Figure 7 PP stacking sections of the initial geology model and the post-production drainage model with the presence of wormholes

Figure 8 shows the stacking sections of PS seismic data of the pre-production reservoir model and the post-production model with the drainage, as well as the difference. In Figure 8b, it is very obvious to distinguish the seismic response of the drainage zone with outstanding peaks and troughs, compared with PP seismic responses. The reasons could rely on 1) there are higher velocity contrasts of S-wave; 2) PS data may have higher resolution due to its relatively short wavelength compared with that of PP data for similar frequencies. Another thing easily seen is that the amplitudes increase with the increase of wormhole density (from left to right, correponding to density changes from 2% to 20%). So do the traveltime delays, which can be observed clearly in Figure 8c. Therefore, it is possible to use converted waves to better image the distribution of wormholes. Further, converted waves can be employed to detect the most likely orientation of wormhole growth, provide a valuable drainage pattern to engineers in the field.

(a) pre-production reservoir   (b) drainage zone with wormhole effects   (c) Difference
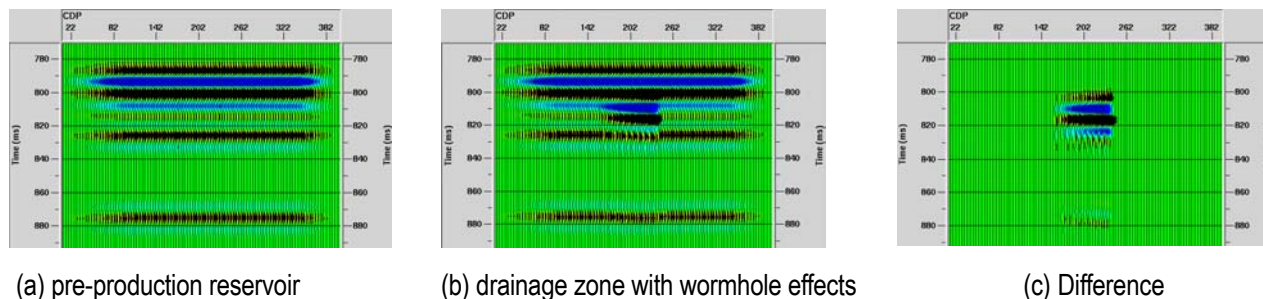
Figure 8 PS stacking sections of the initial geology model and the post-production drainage model with the presence of wormholes

Based on the modelling results, we could conclude that both PP and PS seismic data can be used for imaging the seismic repsonses of the microscopic effects of wormholes. Because of the greater contrasts in V_s, the amplitude anomalies and travel time delays on the PS section are more readily seen than on the PP section, where only subtle changes can be detected around CDP 240 where high wormhole densities exist. We believe the high seismic frequency can help improve the image of microscopic effects of wormholes. The increases in amplitudes from CDP 162 to CDP 242 are proportional to the increase of wormhole density, thus possibly predicting the relations between wormhole distributions and amplitude variations.

References

Chen, S., Lines, L., Embleton, J., Daley, P.F., and Mayo, L., 2003, Seismic detection of cold production footprints of heavy oil in Lloydminster field, the CSEG convention, June, Calgary, Alberta, Canada

Downton, J., 2001, A rock physics framework for interpreting reservoir properties from seismiclly-derived elastic parameters, Scoot Pickford.

Gassmann, F., 1951, Elastic waves through a packing of spheres: Geophysics, 16, 637-685.

Murphy, W., Reischer, A., and Hsu, K., 1993, Modulus decomposition of compressional and shear velocities in sand bodies, Geophysics, 58, P227-239.

Nur, A., Mavko, G., Dvorkin, J., and Galmudi, D., 1998, Critical porosity: a key to relating physical properties to porosity in rocks, The Leading Edge, Marcg, P357-362.

Sawatzky, R.P., Lillico, D.A., London, M.J., Tremblay, B.R. and Coates, R.M., 2002, Tracking cold production footprints, CIPC conference, Calgary, Alberta, Canada.

Tremblay, B., Sedgwick, G., and Vu, D., 1999, A review of cold production in heavy oil reservoirs, EAGE, 10th European Symposium on Improved Oil Recovery, Brighton, UK.